Endocrinology. First published ahead of print July 18, 2013 as doi:10.1210/en.2013-1424

Insulin hypersecretion in islets from diet-induced hyperinsulinemic obese female mice is associated to several functional adaptations in individual beta-cells

Alejandro Gonzalez[1,2], Beatriz Merino[1,2], Laura Marroquí[1,2], Patricia Ñeco[1,2], Paloma Alonso-Magdalena[1,2], Ernesto Caballero-Garrido[1,2], Elaine Vieira[2,3], Sergi Soriano[4], Ramon Gomis[2,3,5], Angel Nadal[1,2], Ivan Quesada[1,2,*]

[1] Instituto de Bioingeniería, Universidad Miguel Hernandez, Elche, Spain.; [2] CIBER de Diabetes y Enfermedades Metabólicas Asociadas (CIBERDEM), Spain.; [3]Diabetes and Obesity Laboratory, IDIBAPS, Barcelona, Spain; [4]Departamento de Fisiología, Genética y Microbiología, Universidad de Alicante, Alicante, Spain.; [5]Hospital Clinic and Universitat de Barcelona, Spain.

Insulin resistance and hyperinsulinemia are generally associated with obesity. Obese non-diabetic individuals develop a compensatory beta-cell response to adjust insulin levels to the increased demand, maintaining euglycemia. Although several studies indicate that this compensation relies on structural changes, the existence of beta-cell functional adaptations is incompletely understood. Here, we fed female mice with high-fat-diet (HFD) for 12 weeks. These animals became obese, hyperinsulinemic, insulin resistant and mild glucose intolerant while fed and fasting glycemia was comparable in HFD and control mice. Islets from HFD animals exhibited increased beta-cell mass and hypertrophy. Additionally, they had enhanced insulin gene expression and content and augmented glucose-induced insulin secretion. Electrophysiological examination of beta-cells from both groups showed no differences in K_{ATP} channel open probability and conductance. However, action potentials elicited by glucose had larger amplitude in obese mice. Glucose-induced Ca^{2+} signals in intact islets, in isolated beta-cells and individual beta-cells within islets were also increased in HFD mice. Additionally, a higher proportion of glucose-responsive cells was present in obese mice. In contrast, whole-cell Ca^{2+} current densities were similar in both groups. Capacitance measurements showed that depolarization-evoked exocytosis was enhanced in HFD beta-cells compared with controls. Although this augment was not significant when capacitance increases of the whole beta-cell population were normalized to cell size, the exocytotic output varied significantly when beta-cells were distributed by size ranges. All these findings indicate that beta-cell functional adaptations are present in the islet compensatory response to obesity.

Obesity is an important risk factor for the development of type 2 diabetes. Insulin resistance and hyperinsulinemia are commonly found in obese individuals, and the relationship and evolution of both factors is involved in the eventual progression from normal glucose tolerance to overt diabetes. Although decreased insulin sensitivity is present in most obese individuals, normal glucose tolerance is preserved in these subjects because insulin resistance is compensated by enhanced pancreatic insulin release, which leads to hyperinsulinemia (1, 2). This adaptation allows for euglycemia or near normoglycemia in these situations (3). However, if the reciprocal β-cell compensation fails to match the increased insulin needs, obese insulin-resistant individuals can progress to impaired glucose tolerance and, eventually, to type 2 diabetes (1, 2). Thus, the adaptation of the β-cell secretory capacity is crucial to avoid impaired glucose homeostasis.

In the progression to diabetes, a gradual decline in β-cell mass and/or function leads to inadequate insulin secretion and increasing plasma glucose levels (2, 4–6).

ISSN Print 0013-7227 ISSN Online 1945-7170
Printed in U.S.A.

Received May 8, 2013. Accepted July 11, 2013.

Abbreviations:

β-cell dysfunction in obese subjects has been associated to glucolipotoxicity or islet amyloid polypeptide among other factors (4, 6–8). In contrast, little is known about the mechanisms allowing for β-cell compensation to obesity, or other insulin-resistance states, and the appearance of hyperinsulinemia. Treatment of rodents with high-fat-diet provides a good experimental model to study β-cell adaptation and failure in obesity (8, 9). Diet-induced obese mice gradually develop insulin resistance, hyperinsulinemia and, if compensatory mechanisms fail, may present hyperglycemia. It has been shown that the adaptation process involves enhanced insulin release. Although numerous studies in both animal models and humans have demonstrated that this augmented secretory response in insulin resistance states is associated with compensatory changes in β-cell mass, the functional adaptation of β-cells remains controversial (1, 8, 10–12). Therefore, in the present study we examined the functional contribution of individual β-cells to the whole insulin secretory response by studying key steps in the stimulus-secretion coupling.

Materials and Methods

Animals, diets and plasma parameters. All protocols were approved by our Animal Ethics Committee according to national regulations. Experiments were performed with C57BL/6J mice. After weaning, 21 d-old female pups were fed for 12 wk with either of the following diets from Research Diets (New Brunswick, NJ, USA): normal diet (ND; 10% fat, 20% protein and 70% carbohydrates; ref.: D12450B) or high fat diet (HFD; 60% fat, 20% protein and 20% carbohydrates; ref.: D12492). Animals were housed in groups of 3 individuals at 22°C and light cycle of 12 h (8.00 am – 8.00 pm). Glucose and insulin plasma levels as well as intraperitoneal glucose tolerance tests (ipGTT) and intraperitoneal insulin tolerance tests (ipITT) were performed as previously published (13). About 15% of mice were resistant to HFD and did not exhibit weight changes compared with controls. These animals were not considered in this study.

Islet isolation and cell culture. Mice were sacrificed at 15 wk old by cervical dislocation and islets were then isolated by collagenase digestion (14). In some experiments, isolated islets were dispersed into single cells by trypsin enzymatic digestion and then cultured overnight at 37°C in RPMI 1640 (Sigma, Madrid, Spain) supplemented with 10% fetal calf serum, 100 IU/ml penicillin, 0.1 mg/ml streptomycin and 11 mM D-glucose (14). Except when indicated, all experiments were done at 37°C.

Quantitative real-time PCR. Quantitative PCR assays were performed using CFX96 Real Time System (Bio-Rad, Hercules, CA), as previously published (15). Primers for insulin were: TTATTGTTTCAACATGGCCC (forward); CAAAGGTGCTGCTTGACAAA (reverse).

Insulin secretion and content measurement

These parameters were analyzed according to protocols published elsewhere (16, 17). Briefly, freshly isolated islets were left to recover in the isolation medium for 2h in the incubator. After recovery, groups of 5 islets were transferred to 400 μl of a buffer solution containing (in mM): 140 NaCl, 4.5 KCl, 2.5 $CaCl_2$, 1 $MgCl_2$, 20 HEPES and the corresponding glucose concentration with final pH at 7.4. Afterwards, 100 μl of the corresponding buffer solution with 5% BSA was added, incubated at room temperature for 3 min and let to cool down for 15 min on ice. Then, the medium was collected and insulin was measured in duplicate samples by radioimmunoassay (RIA) using a Coat-a-Count kit (Siemens, Los Angeles, CA, USA). To obtain insulin content, the islets grouped in batches of 5 were hand-picked and incubated overnight in an ethanol/HCl buffer at 4°C. At the end of the incubation period, the buffer was removed and studied for insulin content. Protein concentration was measured by the Bradford dye method.

Immunocytochemistry, immunohistochemistry and β-cell mass

Pancreas samples were removed and fixed overnight in 4% paraformaldehyde. Subsequently, pancreatic tissue was embedded in paraffin and sections were prepared and stained for β-cell identification according to Montanya et al. (18). For quantification of β-cell area, sections were viewed at a magnification of 20x. The islet cross-sectional area and total pancreatic area was measured using the analysis program Metamorph Software. At least 2 sections, separated by 200 μm were measured per animal. In the case of the immnocytochemistry, insulin-containing cells were identified with monoclonal anti-insulin mouse antibodies (1:200; Sigma) as previously described (14).

Ca^{2+} signaling measurements by fluorescence microscopy and confocal microscopy.Isolated islets and single cells were loaded with either Fura-2 or Fluo-4 (2 μM for cells and 5 μM for islets) for 1 h at room temperature (14). Ca^{2+} signals were recorded using an inverted epifluorescence microscope equipped with 340 and 380 nm band-pass filters (14, 16). Fluorescence records were expressed as the ratio of fluorescence at 340 nm and 380 nm (F340/F380) and the increment of fluorescence (ΔF) was obtained by subtracting the mean basal fluorescence in the absence of stimulus from the fluorescence value during the stimulus. As previously described (17, 19), when the stimuli induced a single Ca^{2+} transient, such as K^+ or the initial response to glucose, we analyzed the maximal amplitude of this transient (ΔF) as an indicator of the Ca^{2+} signal magnitude. Since glucose also induces Ca^{2+} oscillations, we analyzed the area-underthe-curve (AUC) of the whole period of stimulation using Origin software (Origin, Origin Lab Corporation, MA USA). This parameter is an indicator of the global Ca^{2+} increase (19). For the analysis of synchrony as well as the first Ca^{2+} transient with glucose, individual cells within intact islets were monitored using a Zeiss LSM 510 laser confocal microscope (optical section = 8 μm) (14). The Ca^{2+} signal of 4–7 individual β-cells were analyzed in each islet. A synchronized cell within an islet was considered when the analyzed cell exhibited coupling of its Ca^{2+} oscillations with the rest of cells (20, 21). β-cells were identified by their typical Ca^{2+} response to glucose (20, 21).

Patch-clamp recordings. Electrophysiological measurements

were carried out using an EPC-10 USB patch-clamp amplifier in conjunction with the Patch Master Software suite (HEKA Elektronic) or, in the case of K_{ATP} channel experiments, using an Axopatch 200B patch-clamp amplifier in conjunction with the pClamp Software (Axon Instruments Co). Electrodes were made from borosilicate glasses using a P-97 flaming/brown micropipette puller (Sutter Instrument Co) coated with Sylgard 184 (Dow Corning) and polished with a MF-830 microforge (Narishige) and had resistances between 4–6 when filled with the different pipette solutions. Voltage-gated Ca^{2+} currents were measured using the standard whole-cell configuration with a pipette solution containing (in mM): 130 CsCl, 1 $MgCl_2$, 1 $CaCl_2$, 10 EGTA, 3 Mg-ATP and 10 HEPES (pH 7.2 with CsOH). During Ca^{2+} channel measurements, cells were bathed in a medium containing (in mM): 118 NaCl, 10 TEA-Cl, 4.8 CsCl, 1.2 $MgCl_2$, 5 $CaCl_2$ 5 HEPES and 5 D-glucose (pH 7.4 with NaOH). The perforated-patch configuration was used for the membrane potential recordings. The pipette solution contained (in mM): 76 K_2SO_4, 10 NaCl, 10 KCl, 1 $MgCl_2$, 5 HEPES (pH 7.35 with KOH) and 0.24 mg/ml of the pore forming antibiotic Amphotericin B; the bath solution contained (in mM): 140 NaCl, 3.6 KCl, 1.5 $CaCl_2$, 5 $NaHCO_3$, 0.5 $MgSO_4$, 0.5 NaH_2PO_4, 10 HEPES (pH 7.4 with NaOH) and D-glucose as indicated. K_{ATP} channel activity was recorded using standard patch-clamp recording procedures with a pipette solution containing (in mM): 140 KCl, 1$MgCl_2$, 10 HEPES and 1 EGTA (pH 7.2). In these experiments, the bath solution contained (in mM): 5 KCl, 135 NaCl, 2.5 $CaCl_2$, 10 HEPES and 1.1 $MgCl_2$ (pH 7.4) and supplemented with D-glucose as indicated. K_{ATP} channel activity was quantified as previously described (21). Exocytosis was monitored using the standard whole-cell configuration and recording cell capacitance changes through the sine+DC mode of the Lock-In amplifier included in the Patch Master software. For these experiments the pipette solution contained (in mM): 140 CsCl, 10 NaCl, 1 $MgCl_2$, 0.05 EGTA, 3 Mg-ATP, 0.1 cAMP and 5 HEPES (pH 7.2 with CsOH), while bath solution contained (in mM): 118 NaCl, 5.6 KCl, 20 TEA-Cl, 1.2 $MgCl_2$, 5 $CaCl_2$, 5 HEPES and 5 D-glucose (pH 7.4 with NaOH). Only experiments with stable and low access resistance and small leak currents were used. The seal resistance value was typically $>$ 3MΩ. No differences were allowed between ND and HFD groups in any of these parameters. K_{ATP} channel experiments were carried out at room temperature (20–24°C). All the other experiments were carried out at physiological temperature (34–36°C). β-cells were identified by their electrical response to glucose and steady state inactivation of Na^+ currents (22; Supplemental Figure 1).

Statistical analysis. Data is shown as mean ± SE. Student's *t* test or one-way ANOVA with Bonferroni correction were performed with a level of significance $P < .05$.

Results

Obese mice exhibit increased body weight and hyperinsulinemia. Female mice were fed with either high fat (HFD) or normal diet (ND) for 12 wk. At the end of both treatments, HFD mice displayed increased body weight and fed hyperinsulinemia compared to controls (Figure 1A-B), while glycemia in fed state remained similar (Figure 1C). When mice were subjected to ipGTT, initial fasting plasma glucose levels showed a very mild increase in obese mice (ND = 95.4 ± 4.4 mg/dl; HFD = 105.9 ± 3.4 mg/dl) (Figure 1D). Obese mice presented glucose intolerance at 15 and 30 min, yet glucose values were found similar after 2 h of the glucose load (Figure 1D). Additionally, analysis of ipITT revealed decreased insulin sensitivity for HFD mice (Figure 1E). To further check for this insulin resistance, plasma glucose and insulin levels were measured before an intraperitoneal glucose load and after 30 min (Figure 1F and G). These experiments showed that HFD mice were hyperinsulinemic at 0 and 30 min compared with controls, while glucose levels remained similar in both groups. All these results are compatible with a model of HFD-induced obesity with insulin resistance and moderate glucose intolerance, in which plasma glucose levels remained near normoglycemia at the expense of increased plasma insulin levels.

High-fat diet leads to increased β-cell mass and β-cell hypertrophy. Hyperinsulinemia has been frequently asso-

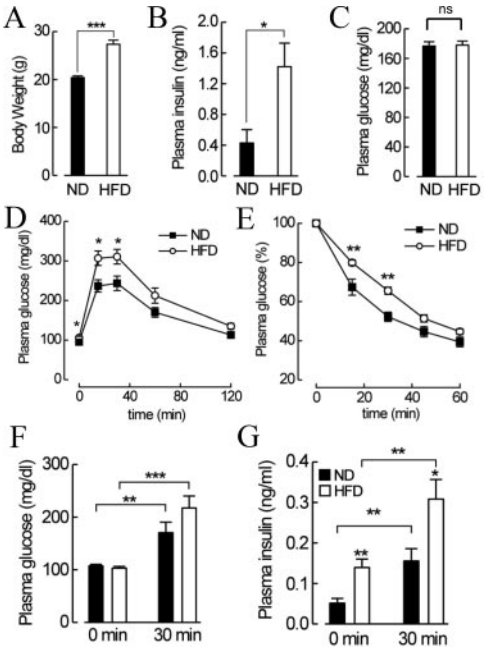

Figure 1. Metabolic features in HFD and control mice. A: Body weight (n = 10 and 13 mice for ND and HFD, respectively). Fed plasma insulin (B; n = 8 mice for each group) and glucose (C; n = 9 and 12 mice for ND and HFD, respectively) in mice submitted to normal and high fat diet. Glucose tolerance test (D; n = 11 and 12 mice for ND and HFD, respectively) and insulin tolerance test (E; n = 6 mice for each group). Obese and lean mice were subjected to an intraperitoneal glucose load and then, plasma glucose (F) and insulin levels (G) were measured at 0 and 30 min (n = 6 and 8 mice for ND and HFD, respectively). ND: Normal diet; HFD: high fat diet. Statistically significant: *; $P < .05$; **, $P < .01$; ***, $P < .001$; ns, non significant.

ciated with enhanced β-cell mass in obesity models (2). As shown in Figure 2A-C, the pancreas size and relative and absolute β-cell mass were found bigger in obese mice. Since the involvement of β-cell size is still controversial (7, 8, 10), we evaluated this parameter by different approaches: average area occupied per single β-cell in islets from pancreas sections (Figure 2D), cell size estimated from single β-cell membrane capacitance compensation during electrophysiological recordings (Figure 2E) and β-cell diameter analysis in immuno-identified isolated β-cells (Figure 2F,G). β-cell size measurements were similar to those previously reported (23, 24). All these experiments indicated that β-cell hypertrophy was present during diet-induced obesity.

Pancreatic islets from obese mice show enhanced insulin release in response to glucose. Insulin gene expression as well as insulin protein content were increased in pancreatic islets from obese mice compared with controls (Figure 3A,B). When the islet secretory capacity was analyzed in vitro, we also observed enhanced insulin release in response to glucose in obese mice (Figure 3C-D). Thus, these findings indicate that hyperinsulinemia in obese mice may be associated to the enhanced secretory capacity of their islets. Since there is not much information about the mechanisms involved in this hypersecretion, the next experiments were designed to analyze the main signaling events involved in β-cell insulin release.

Action potentials during glucose stimulation have higher amplitude in β-cells from HFD mice. K_{ATP} channels play a central role in coupling metabolic changes to β-cell excitability and insulin secretion. Cell-attached measurements revealed that K_{ATP} channel open probability in response to glucose was similar in β-cells from both groups (Figure 4A,B). This finding was further supported when the K_{ATP} channel slope conductance was analyzed through the application of voltage ramps in the perforated-patch voltage-clamp configuration (Figure 4C). In this case, slope conductance values normalized to cell capacitance in response to 3 and 8 mM glucose as well as tolbutamide were similar between both groups (Figure 4D). Thus, glucose-induced changes in K_{ATP} channel activity are unlikely to play a major role in the insulin secretion differences observed in obese mice. Consistent with this, the characteristic glucose-induced hyperpolarization of the mitochondrial membrane potential (Ψm) was found similar in both groups (Supplemental Figure 2), suggesting a comparable mitochondrial activation in HFD and control islets in response to glucose.

Perforated-patch recordings allowed us to study plasma membrane potential changes in response to glucose without disturbing the intracellular milieu. These experiments showed that resting membrane potential at 3 mM glucose was virtually identical among both groups (ND= –78 ± 0.7 mV; HFD= –78 ± 1.0 mV) (Figure 4E,F). Upon stimulation with 8 mM glucose, β-cells from obese and lean mice depolarized to similar values (ND= –43 ± 1.0 mV; HFD= –45 ± 1.0 mV). These membrane potential levels are characterized by the appearance of action potentials in both groups (Figure 4E,G). Interestingly, while no significant differences existed in the firing frequency (Figure 4H) or the action potential duration (data not shown), the peak amplitude of action potentials was largely enhanced by ≈35% in β-cells from HFD mice compared with controls (Figure 4I,J), leading to peak voltages of 3.7 ± 2.0 mV and –6.9 ± 2.0 mV, respectively.

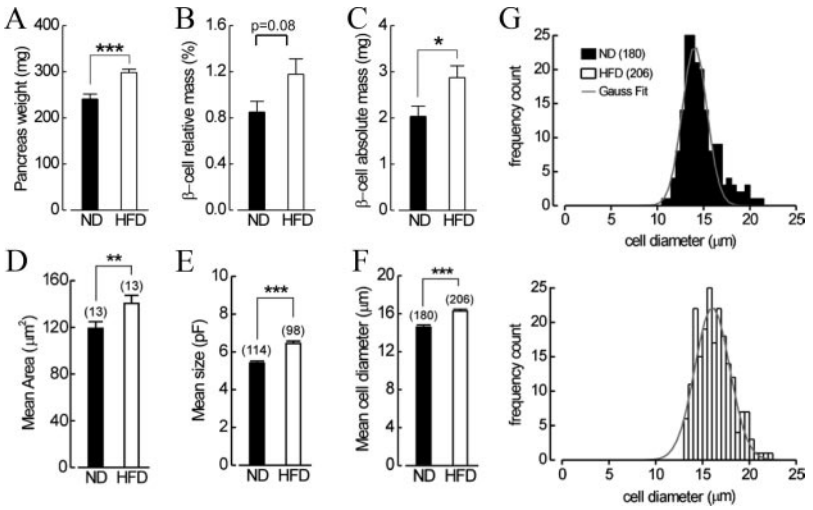

Figure 2. Structural changes in obese mice compared with controls. Pancreas weight (A), relative (B) and absolute (C) β-cell mass as well as β-cell cross-sectional area (D) was quantified in both groups by immunohistochemistry in pancreas sections. At least 300 islets from 5–7 different pancreases were analyzed in each condition. β-cell mean size in HFD and ND mice was also evaluated by electrophysiology from capacitance measurements (E) and by image analysis from immunoidentified β-cells isolated in culture (F). In the former case, cell size was expressed in pF (23). G: Normalized size distribution frequency of experiments shown in F. The numbers in parenthesis indicate the number of analyzed cells. ND: Normal diet; HFD: high fat diet; pF: picofarads. Statistically significant: **, $P < .01$ comparing ND and HFD; ***, $P < .001$.

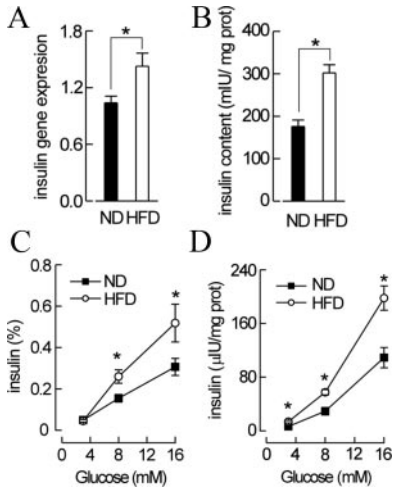

Figure 3. Insulin secretion, content and gene expression in obese and lean mice. Insulin gene expression from isolated islets from HFD and ND mice was analyzed by real-time PCR (A; n = 13 and 8 samples, respectively) while insulin content by RIA (B; n ≥ 12 samples per condition). Insulin content was normalized to total protein content. C, D: Insulin release in response to 3, 8 and 16 mM glucose was measured by RIA in isolated islets from both groups. Insulin secretion was expressed as the percentage of insulin content (C) or normalized to total protein content (D) (n= n ≥ 12 samples per condition). ND: Normal diet; HFD: high fat diet. Statistically significant: *; $P < .05$.

β-cells from obese mice have enhanced Ca^{2+} signals in response to glucose. To study Ca^{2+} dynamics in intact islets from both models, we measured intracellular Ca^{2+} signals by Fura-2 and fluorescence microscopy. As shown in Figure 5A, exposure of islets to both 8 and 16 mM glucose produced a transient Ca^{2+} rise followed by oscillations in both groups. However, in the case of HFD islets, the Ca^{2+} response resulted in a higher amplitude of the transient rise as well as increased area-underthe-curve (AUC) of the whole signal (Figure 5B,C). Unlike glucose, a nonmetabolic stimulus such as K^+ did not lead to different responses (Figure 5D,E). Glucose induced similar effects in isolated β-cells in culture (Figure 5F and Supplemental Figure 3). In these experiments, we also observed that the percentage of cells responding to glucose was increased in obese mice (Figure 5G). Finally, to further check whether enhanced islet Ca^{2+} responses were due to improved Ca^{2+} signals in individual β-cells, we studied single cells by confocal microscopy in thin optical slices (<8 μm) within intact islets. As shown in figure 5H,I, glucose-induced Ca^{2+} signals in individual β-cells were also enlarged in HFD mice. Unlike amplitude and AUC, the oscillatory frequency was similar in both groups at 11 mM glucose (1.53 ± 0.8 oscillations/min and 1.54 ± 0.8 oscillations/min in ND and HFD; n = 19 and 54 cells, respectively). Since insulin secretion also relies on the efficiency of cell-to-cell coupling (20), we analyzed the synchrony of oscillatory Ca^{2+} signals among cells. However, no major differences were found between both groups (Supplemental Figure 4). In order to study modifications in the voltage-dependent Ca^{2+} currents, we then performed standard whole-cell patch-clamp measurements in isolated β-cells from both groups. The peak Ca^{2+} currents as well as the Ca^{2+} charge transfer were found larger in β-cells from obese mice (Figure 5J and Supplemental Figure 5). However, these differences disappeared when these parameters were normalized to cell capacitance (Figure 5K). It has been reported that fatty acids increases L-type Ca^{2+} channels (25, 26). In both models, the contribution of these channels to the Ca^{2+} currents was comparable, since the blocker nifedipine led to similar inhibition (Supplemental Figure 6).

Exocytotic responses in β-cells from HFD mice and controls. Simultaneous measurements of depolarization-evoked capacitance changes and Ca^{2+} currents were used to study diet effects on exocytosis (27). β-cells were subjected to a train of ten 500ms voltage depolarizations from –70 to 0 mV (Figure 6A,B). This protocol leads to further expansion of the Ca^{2+} microdomains associated with the

release of the ready releasable pool (RRP) and triggers the recruitment of deeper granules (28). These experiments led to enhanced exocytotic responses in HFD in regard to the early (first two pulses) as well as late (pulses from 3 to 10) components of the exocytosis (Figure 6C). Due to the increased β-cell size in HFD, these differences were not significant when normalized to this parameter (Figure 6D). We also performed experiments with 50 ms pulses (Figure 6E,F). This action potential-like stimulation is tightly related to the release of granules that are attached to Ca^{2+} channels (28). Similar results were obtained as those observed for 500 ms (Figure 6E,F). In both types of stimulation, integrated Ca^{2+}-currents normalized to cell size elicited during each pulse as well as the exocytosis Ca^{2+} efficiency were not significantly different between both groups (Supplemental Figure 7). The capacitance voltage-dependence was also similar in both groups, although some values between -10mV and 10mV tended to be higher in HFD (Figure 6G,H). When we considered the whole population, which showed an ample cell size dispersion (Figure 6I,J), no significant differences between both groups were found in the normalized capacitance increase (Figure 6D,F), suggesting that the enhanced capacitance responses in HFD β-cells were likely due to their increased cell size. However, interestingly, when maximal capacitance increases in response to 500ms pulses were plotted against cell size (Figure 6I-K), this correlation was not obvious, showing that bigger cells tended to secrete with less efficiency. Actually, when cells were separated in size ranges (Figure 6K), we found that the exocytotic response of β-cells within 5 and 6.5 pF was higher in obese mice compared with both control cells of the same range and the bigger HFD cells. This effect was more pronounced in the reserve pool (Figure 6K). These results indicate that HFD β-cell exocytosis behavior might be heterogeneous depending on cell size.

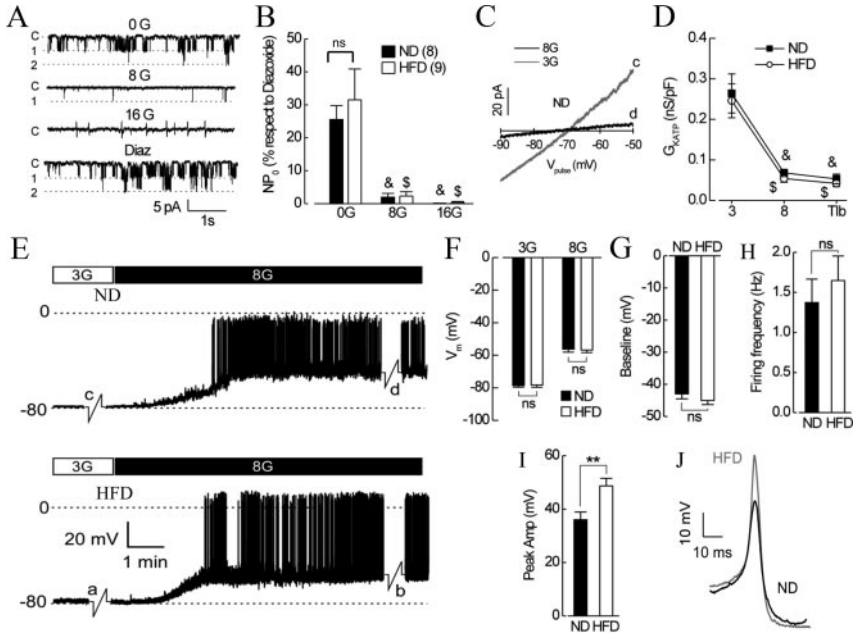

Figure 4. Glucose-stimulated K_{ATP} channel activity and membrane potential in β-cells from HFD and control mice. A: Representative example of K_{ATP} channel activity in response to 0, 8 and 16 mM glucose as well as 100 μM diazoxide in an isolated HFD β-cell. Channel activity was measured by patch-clamp in cell-attached configuration. B: K_{ATP} channel open probability obtained from 8 cells of control mice and 9 cells of HFD mice. C: The membrane potential was ramped from –100 to 0 mV to estimate the slope conductance of β-cells in different conditions. The graph illustrates the current-voltage relationship in a control β-cell during these voltage ramps. D: Slope conductance normalized to membrane capacitance was obtained from the linear part (between –100 and –50 mV) of the current-voltage relationship shown in C in isolated β-cells from both groups (n = 15 isolated cells for each group). E: Representative examples of membrane potential variations in response to 8 mM glucose in both groups of mice. These recordings were obtained by perforated-patch current-clamp. Letters (a-d) indicate the times when the voltage ramp protocols shown in C and D were obtained. F: Membrane potential at 3 and 8 mM glucose is shown for both groups. Several parameters related with the action potentials were also compared in both groups: baseline membrane potential from which arose action potentials (G), firing frequency (H) and peak amplitude (I) (n = 16 and 13 isolated cells for ND and HFD, respectively). J: Two representative β-cell action potentials from ND and HFD mice, respectively, are illustrated for comparison. G: glucose; Diaz: diazoxide; Tlb: tolbutamide; ND: Normal diet; HFD: high fat diet. Statistically significant comparing ND and HFD: *; $P < .05$. Statistically significant comparing with ND control: &, $P < .05$. Statistically significant comparing with HFD control: $, $P < .05$. NS: nonsignificant.

Discussion

During prediabetic stages in obesity, compensatory β-cell changes oppose to insulin resistance, allowing for normoglycemia. However, when this adaptation fails, progression to hyperglycemia and frank diabetes may eventually occur (2, 4–6). The mechanisms involved in β-cell dysfunction and diabetes development have received much attention. Yet, less is known about the processes participating in β-cell compensatory changes in prediabetic stages. In both animals and humans, the increase in β-cell mass is critical in this adaptative response in obesity (5,10–12,29). However, the exact contribution of β-cell functional changes is still unclear (1, 2, 11, 12). In the present study, we showed that female mice subjected to HFD for 12 wk exhibit moderate glucose intolerance and insulin resistance as well as hyperinsulinemia. Given that fed and fasting plasma glucose levels in HFD mice were not much different

to those of lean controls, it indicates that plasma glucose concentrations were maintained near normoglycemia at the expense of an increased insulin output, suggesting an adaptative compensatory response. Consistent with this, we observed increased plasma insulin levels before and after a glucose load in HFD mice compared with lean controls (Figure 1). It has been shown that HFD protocols can lead to different metabolic outcomes in male mice compared to those described here in females, leading to β-cell dysfunction and overt hyperglycemia (4, 6). However, it has been previously reported that female mice are protected against HFD, insulin resistance and progression to diabetes (30, 31). Actually, we chose female mice because it has been suggested to provide a better model to study the initial prediabetic stages of the compensatory response (9, 32). This is likely related with the protective effect of estrogens (30, 31). It has been shown that chronic estradiol administration in wild-type ovariectomized mice exerts a beneficial effect against HFD induced glucose intolerance, while these actions do not occur in estrogen receptor alpha knockout mice (30). Similar protective effects have been reported in animal models of insulin deficient diabetes (31). Additionally, compared with other strains, C57BL/6J mice are more resistant to diet-induced obesity, which allows a better characterization of prediabetic conditions. Differences in the protocols used for the dietary treatment may also lead to variances in β-cell phenotypes in males and females during obesity. Given that the exposure to HFD started at 3 wk old, we cannot discard that, in addition to functional changes, the diet also affected β-cell growth processes.

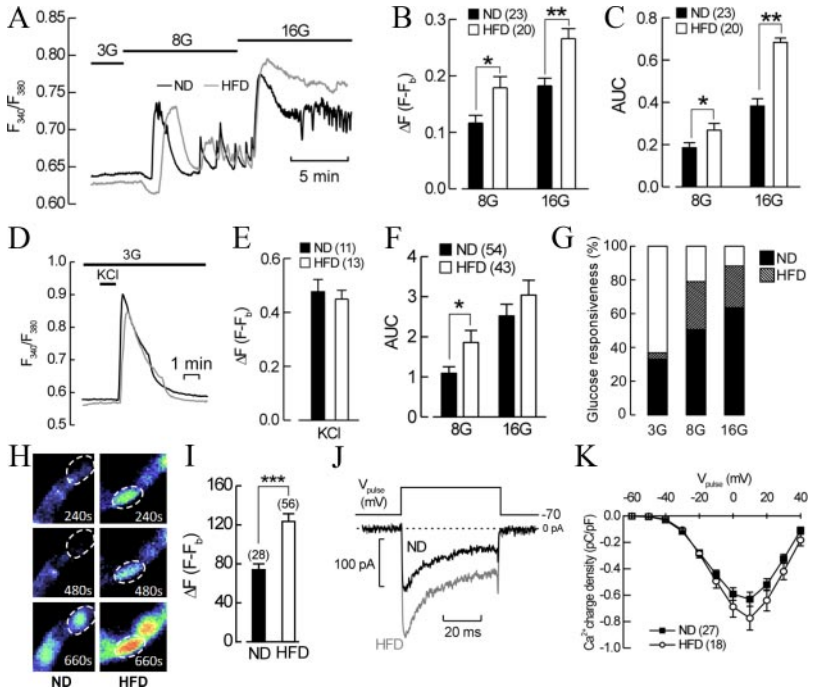

Figure 5. Glucose-induced Ca^{2+} signaling in β-cells of obese and control mice. A: Intracellular Ca^{2+} signals were measured in intact islets by conventional fluorescence microscopy and Fura-2. Two examples of the Ca^{2+} signal are illustrated for both groups in response to 8 and 16 mM glucose. B: Analysis of the fluorescence increase (ΔF) during the first Ca^{2+} transient in response to 8 and 16 mM glucose. C: Analysis of the area under the curve (AUC) of the whole stimulation period as a global indicator of the Ca^{2+} signal during the stimulus. D: Two examples of the Ca^{2+} signal are illustrated for both groups in response to depolarization induced by 75 mM KCl. E: Analysis of the fluorescence increase (ΔF) during the Ca^{2+} transient in response to KCl. F: Area under the curve (AUC) of the whole stimulation period in response to glucose in isolated islet cells in culture. G: Percentage of responsive cells to glucose in isolated β-cells of obese mice and controls (n = 54 and 43 isolated β-cells for ND and HFD, respectively). H: Ca^{2+} signals in individual β-cells were measured in thin optical sections (8 μm) of intact islets by confocal microscopy and Fluo-4. The images show the fluorescence increase in response to glucose during a Ca^{2+} signal in individual cells from a control mice (left) or obese (right). I: Fluorescence increase (ΔF) during the first Ca^{2+} transient in response to 11 mM glucose in individual cells within islets from experiments shown in H. J: Ca^{2+} currents in β-cells from both groups in response to a depolarizing pulse from –70 mV. K: Ca^{2+} current densities versus voltages in β-cells of obese and lean mice. The numbers in parenthesis indicate the number of analyzed cells. G: glucose; ND: Normal diet; HFD: high fat diet; F: fluorescence; F_b: basal fluorescence. Statistically significant: *; $P < .05$; **, $P < .01$; ***, $P < .001$.

Increased β-cell mass is a hallmark of the islet adaptative response to obesity and it has been mainly associated to hyperplasia (7, 8, 10). In agreement with this, we observed that β-cell mass was enlarged in HFD mice (Figure 2). Interestingly, while others have not found changes in β-cell size in HFD models (7), we showed here that obese mice exhibited β-cell hypertrophy, indicating that this is also a key process in the β-cell structural adaptations to obesity. Additionally, we show that isolated islets from obese mice displayed higher insulin gene expression and protein content as well as enhanced secretory output in response to glucose compared with controls (Figure 3). Few studies in diet-induced obese mice or insulin-resistant states have suggested that changes in islet metabolism may account for the augmented insulin secretion (8, 9, 32, 33). However, if a metabolic change was present in our experiments, it did not affect the K_{ATP} channel activity, the K_{ATP} channel slope conductance or the plasma membrane potential in response to glucose. Actually, most differences observed in this study were found down-stream of K_{ATP} channels. In any case, several glucose-derived metabolic factors different from ATP such as NADH and

glutamate have been involved as intracellular mediators of glucose-induced insulin secretion (34, 35). In addition to diet-induced obese mice, an increased secretory performance has been also reported in obese Zucker fatty rats (1). In contrast, other studies have shown that β-cell compensation relies mainly on structural adaptations rather than changes in the secretory efficiency (10, 12). In part, these discrepancies might be probably due to the different metabolic outputs that are obtained depending on the mice gender, diet fat content as well as duration and life periods of the dietary treatment (36).

In addition to structural changes, the present study shows that the compensatory response during prediabetic early stages in obesity is also sustained by β-cell functional changes at different levels, probably down-stream of K_{ATP} channels, as commented earlier. Interestingly, β-cells from obese mice exhibited action potentials of larger amplitude (Figure 4I,J). If we take into account the difference in the plasma membrane potential voltages achieved by both groups and the voltage-dependence of Ca^{2+} currents (Figure 5K) and exocytosis (Figure 6H), we should expect that action potentials fired by HFD β-cells lead to increased Ca^{2+}-currents and exocytosis. This may explain the enhanced Ca^{2+} signals and glucose-induced insulin release in HFD β-cells (Figure 3 and 5). It is noteworthy to mention that recent work has shown that pharmacological inhibition of BK channels leads to taller action potentials, which increases Ca^{2+} currents, Ca^{2+} signals and insulin release (37–39). Consistent with this, the use of a BK channel blocker leads to enhanced Ca^{2+} responses in islets from normal mice (P. Ñeco, B. Merino, A. Gonzalez, A. Nadal, I. Quesada, unpublished preliminary results). Thus, although this possibility would require further investigation, it is tempting to speculate that modifications at the level of these channels might be involved in the larger action potentials observed in HFD β-cells.

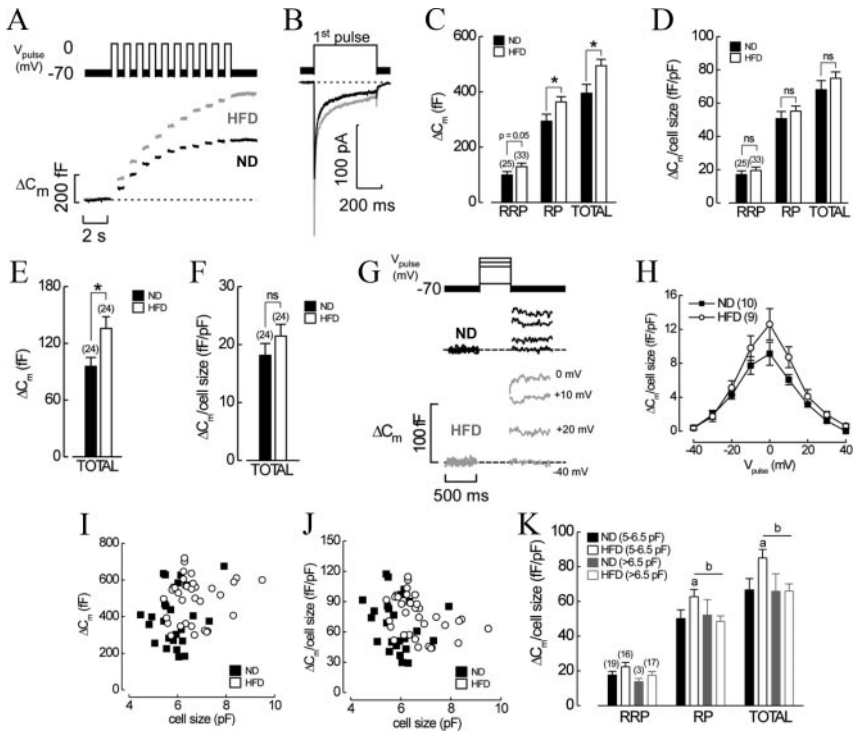

Figure 6. Exocytotic responses in β-cells from obese and lean mice. A: Examples of exocytotic responses to ten 500 ms depolarizing pulses (from –70 to 0 mv) in HFD and control β-cells. B: Representative Ca^{2+} currents elicited during the first depolarizing pulse in experiments shown in A. C: Average capacitance increase for the ready releasable pool (RRP; first two pulses; (23)), the reserve pool (RP) and for all the depolarizing pulses (total). D: As in C but normalized to cell size. E: Average capacitance increase after stimulation with fifteen 50 ms depolarizing pulses. F: As in E but normalized to cell size. G: Representative exocytotic responses to 500 ms depolarizing pulses from –70 mV to –40, 0, +10 and +20 mV. H: Voltage-dependence of normalized capacitance increase in HFD and control β-cells. I: Maximal capacitance increases in response to ten 500 ms depolarizing pulses versus cell size (n = 25 and 33 isolated cells for ND and HFD, respectively). J: As in I but normalized to cell size. K: Normalized capacitance increase from experiments in J, but separated in cell size ranges (size ranges which prevented differences in this parameter between groups): 5–6.5 pF (n = 19 and 16 cells for control and HFD mice, respectively) and > 6.5 pF (n = 3 and 17 cells for control and HFD mice, respectively). Numbers in parenthesis indicate the number of analyzed cells. ND: Normal diet; HFD: high fat diet. Statistically significant: *, a, b, $P < .05$; ns: nonsignificant.

Analysis of glucose-induced Ca^{2+} signals in intact islets, in individual β-cells within islets and isolated cells in culture revealed enhanced Ca^{2+} responses in obese mice. Additionally, higher cell recruitment in response to glucose was observed in HFD. The voltage-dependence of β-cell exocytosis correlates very well to that of the inward Ca^{2+} currents and the magnitude of the Ca^{2+} signals (40). Thus, it is expected that a higher Ca^{2+} entry trough voltage-dependent Ca^{2+}-channels would lead to enhanced Ca^{2+} signals as a trigger for exocytosis, resulting in more secretion. When Ca^{2+} current densities were evaluated in conditions where cell metabolism is not preserved, no major differences were found between HFD and controls. Similarly, a nonmetabolic stimulus such as KCl did not produce Ca^{2+} signal differences. Thus, it is likely that a metabolism product may be involved with the glucose-induced changes in HFD mice. In this regard, it has been reported that glucose-derived molecules such as ATP, NADH or glutamate are involved in glucose-induced insulin secretion by modulation of voltage-gated K^+ (K_v) or

Ca^{2+} channels or the exocytotic machinery (35, 41–45).

The exocytotic response of each individual β-cell from HFD was enhanced respect to controls (Figure 6). These differences disappeared when capacitance increases were normalized to cell size, suggesting that the exocytotic efficiency was comparable in both groups while the absolute secretory response may be related with the hypertrophy found in HFD β-cells (Figure 2). However, in the case that similar exocytotic efficiency would be present in both models, the taller action potentials and increased Ca^{2+} signals as well as the bigger cell size in HFD β-cells would lead to enhanced secretion. Actually, increased insulin output was observed in HFD islets compared to controls (Figure 3). Intriguingly, a clear correspondence between maximal capacitance increase and cell size was not found. In fact, medium-size HFD β-cells seemed to be more vigorous in terms of secretion compared with both bigger HFD cells and control medium-size cells. This observation also points to an enhanced secretion in obese mice. Heterogeneous secretion depending on cell size has been previously observed in β-cells (24). This could be an interesting aspect since it may suggest that increased exocytosis in medium-size β-cells may result from an adaptative response to obesity. In contrast, given that hypertrophy has been associated to β-cell dedifferentiation and senescence (46–48), bigger β-cells might be less efficient or lose the adaptative response. In this regard, it would be interesting to study how this heterogeneity in cell size and exocytosis evolves during obesity and its relationship with the onset of diabetes.

In summary, in the present study we show that, in addition to the well-known compensatory changes in β-cell mass during prediabetic stages in obesity, β-cells develop hypertrophy and, independently, several functional adaptations, all of which may allow, individually or cooperatively, for the enhanced glucose-induced insulin-release shown here. These functional changes consist of higher action potentials, augmented Ca^{2+} signals and cell recruitment as well as more efficient exocytosis in middle-size β-cells. Whether these compensatory adaptations could be manipulated, it would be of interest for the design of therapeutic strategies against hyperglycemia and diabetes.

Acknowledgments

The authors thank M.S. Ramon and M.L. Navarro for their expert technical assistance.

Address all correspondence and requests for reprints to: * I. Quesada. Instituto de Bioingeniería, Universidad Miguel Hernández, Avenida de la Universidad s/n, 03202 Elche, Spain. Phone: (+34) 96 522 2003 Email: ivanq@umh.es.

Disclosure Summary: The authors have nothing to disclose.

This work was supported by grants from the Ministerio de Ciencia e Innovación (BFU2010–21773; BFU2011–28358; SAF2010–19527), Generalitat Valenciana (PROMETEO/2011/080; ACOMP/2013/022), Generalitat de Catalunya (2009 SGR 1426) and European Foundation for the Study Diabetes (EFSD/BI Basic Programme). CIBERDEM is an initiative of the Instituto de Salud Carlos III.

References

1. **Kargar C, Ktorza A.** Anatomical versus functional beta-cell mass in experimental diabetes. *Diabetes Obes Metab 10 Suppl*. 2008;4:43–53.
2. **Kahn SE, Hull RL, Utzschneider KM.** Mechanisms linking obesity to insulin resistance and type 2 diabetes. *Nature*. 2006;444:840–846.
3. **Weir GC, Bonner-Weir S.** Five stages of evolving beta-cell dysfunction during progression to diabetes. *Diabetes 53 Suppl*. 2004;3:S16–21.
4. **Collins SC, Hoppa MB, Walker JN, Amisten S, Abdulkader F, Bengtsson M, Fearnside J, Ramracheya R, Toye AA, Zhang Q, Clark A, Gauguier D, Rorsman P.** Progression of diet-induced diabetes in C57BL6J mice involves functional dissociation of Ca2(+) channels from secretory vesicles. *Diabetes*. 2010;59:1192–1201.
5. **Sachdeva MM, Stoffers DA.** Minireview: Meeting the demand for insulin: molecular mechanisms of adaptive postnatal beta-cell mass expansion. *Mol Endocrinol*. 2009;23:747–758.
6. **Peyot ML, Pepin E, Lamontagne J, Latour MG, Zarrouki B, Lussier R, Pineda M, Jetton TL, Madiraju SR, Joly E, Prentki M.** Beta-cell failure in diet-induced obese mice stratified according to body weight gain: secretory dysfunction and altered islet lipid metabolism without steatosis or reduced beta-cell mass. *Diabetes*. 2010;59:2178–2187.
7. **Matveyenko AV, Gurlo T, Daval M, Butler AE, Butler PC.** Successful versus failed adaptation to high-fat diet-induced insulin resistance: the role of IAPP-induced beta-cell endoplasmic reticulum stress. *Diabetes*. 2009;58:906–916.
8. **Sone H, Kagawa Y.** Pancreatic beta cell senescence contributes to the pathogenesis of type 2 diabetes in high-fat diet-induced diabetic mice. *Diabetologia*. 2005;48:58–67.
9. **Reimer MK, Ahren B.** Altered beta-cell distribution of pdx-1 and GLUT-2 after a short-term challenge with a high-fat diet in C57BL/6J mice. *Diabetes 51 Suppl*. 2002;1:S138–143.
10. **Hull RL, Kodama K, Utzschneider KM, Carr DB, Prigeon RL, Kahn SE.** : Dietary-fat-induced obesity in mice results in beta cell hyperplasia but not increased insulin release: evidence for specificity of impaired beta cell adaptation. *Diabetologia*. 2005;48:1350–1358.
11. **Seino S, Shibasaki T, Minami K.** Dynamics of insulin secretion and the clinical implications for obesity and diabetes. *J Clin Invest*. 2011;121:2118–2125.
12. **Terauchi Y, Takamoto I, Kubota N, Matsui J, Suzuki R, Komeda K, Hara A, Toyoda Y, Miwa I, Aizawa S, Tsutsumi S, Tsubamoto Y, Hashimoto S, Eto K, Nakamura A, Noda M, Tobe K, Aburatani H, Nagai R, Kadowaki T.** Glucokinase and IRS-2 are required for compensatory beta cell hyperplasia in response to high-fat diet-induced insulin resistance. *J Clin Invest*. 2007;117:246–257.
13. **Bonora E, Manicardi V, Zavaroni I, Coscelli C, Butturini U.** Relationships between insulin secretion, insulin metabolism and insulin resistance in mild glucose intolerance. *Diabete Metab*. 1987;13:116–121.
14. **Quesada I, Todorova MG, Alonso-Magdalena P, Beltra M, Carneiro EM, Martin F, Nadal A, Soria B.** Glucose induces opposite

intracellular Ca2+ concentration oscillatory patterns in identified alpha- and beta-cells within intact human islets of Langerhans. *Diabetes*. 2006;55:2463–2469.
15. **Marroqui L, Vieira E, Gonzalez A, Nadal A, Quesada I.** Leptin downregulates expression of the gene encoding glucagon in alphaTC1–9 cells and mouse islets. *Diabetologia*. 2011;54:843–851.
16. **Alonso-Magdalena P, Vieira E, Soriano S, Menes L, Burks D, Quesada I, Nadal A.** Bisphenol A exposure during pregnancy disrupts glucose homeostasis in mothers and adult male offspring. *Environ Health Perspect*. 2010;118:1243–1250.
17. **Alonso-Magdalena P, Ropero AB, Carrera MP, Cederroth CR, Baquie M, Gauthier BR, Nef S, Stefani E, Nadal.** A Pancreatic insulin content regulation by the estrogen receptor ER alpha. *PLoS One*. 2008;3:e2069.
18. **Montanya E, Tellez N.** Pancreatic remodeling: beta-cell apoptosis, proliferation and neogenesis, and the measurement of beta-cell mass and of individual beta-cell size. *Methods Mol Biol*. 2009;560:137–158.
19. **Rafacho A, Marroqui L, Taboga SR, Abrantes JL, Silveira LR, Boschero AC, Carneiro EM, Bosqueiro JR, Nadal A, Quesada I.** Glucocorticoids in Vivo Induce Both Insulin Hypersecretion and Enhanced Glucose Sensitivity of Stimulus-Secretion Coupling in Isolated Rat Islets. *Endocrinology*. 2010;151:85–95.
20. **Nadal A, Quesada I, Soria B.** Homologous and heterologous asynchronicity between identified alpha-, beta- and delta-cells within intact islets of Langerhans in the mouse. *J Physiol*. 1999;517:85–93.
21. **Soriano S, Gonzalez A, Marroqui L, Tuduri E, Vieira E, Amaral AG, Batista TM, Rafacho A, Boschero AC, Nadal A, Carneiro EM, Quesada I.** Reduced insulin secretion in protein malnourished mice is associated with multiple changes in the beta-cell stimulus-secretion coupling. *Endocrinology*. 2010;151:3543–3554.
22. **Göpel S, Kanno T, Barg S, Galvanovskis J, Rorsman P.** Voltage-gated and resting membrane currents recorded from B-cells in intact mouse pancreatic islets. *J Physiol*. 1999;521:717–728.
23. **Barg S, Galvanovskis J, Göpel SO, Rorsman P, Eliasson L.** Tight coupling between electrical activity and exocytosis in mouse glucagon-secreting alpha-cells. *Diabetes*. 2000;49:1500–10.
24. **Leung YM, Ahmed I, Sheu L, Tsushima RG, Diamant NE, Hara M, Gaisano HY.** Electrophysiological characterization of pancreatic islet cells in the mouse insulin promoter-green fluorescent protein mouse. *Endocrinology*. 2005;146:4766–4775.
25. **Olofsson CS, Salehi A, Holm C, Rorsman P.** Palmitate increases L-type Ca2+ currents and the size of the readily releasable granule pool in mouse pancreatic beta-cells. *J Physiol*. 2004;557:935–948.
26. **Tian Y, Corkey RF, Yaney GC, Goforth PB, Satin LS, Moitoso de Vargas L.** Differential modulation of L-type calcium channel subunits by oleate. *Am J Physiol Endocrinol Metab*. 2008;294:E1178–1186.
27. **Kanno T, Ma X, Barg S, Eliasson L, Galvanovskis J, Gopel S, Larsson M, Renstrom E, Rorsman P.** Large dense-core vesicle exocytosis in pancreatic beta-cells monitored by capacitance measurements. *Methods*. 2004;33:302–311.
28. **Hoppa MB, Collins S, Ramracheya R, Hodson L, Amisten S, Zhang Q, Johnson P, Ashcroft FM, Rorsman P.** Chronic palmitate exposure inhibits insulin secretion by dissociation of Ca(2+) channels from secretory granules. *Cell Metab*. 2009;10:455–465.
29. **Butler AE, Janson J, Soeller WC, Butler PC.** Increased beta-cell apoptosis prevents adaptive increase in beta-cell mass in mouse model of type 2 diabetes: evidence for role of islet amyloid formation rather than direct action of amyloid. *Diabetes*. 2003;52:2304–2314.
30. **Riant E, Waget A, Cogo H, Arnal JF, Burcelin R, Gourdy P.** Estrogens protect against high-fat diet-induced insulin resistance and glucose intolerance in mice. *Endocrinology*. 2009;150:2109–2117.
31. **Tiano J, Mauvais-Jarvis F.** Selective estrogen receptor modulation in pancreatic beta-cells and the prevention of type 2 diabetes. *Islets*. 2012;4:173–176.
32. **Fex M, Nitert MD, Wierup N, Sundler F, Ling C, Mulder H.** Enhanced mitochondrial metabolism may account for the adaptation to insulin resistance in islets from C57BL/6J mice fed a high-fat diet. *Diabetologia*. 2007;50:74–83.
33. **Chen C, Hosokawa H, Bumbalo LM, Leahy JL.** Mechanism of compensatory hyperinsulinemia in normoglycemic insulin-resistant spontaneously hypertensive rats. Augmented enzymatic activity of glucokinase in beta-cells. *J Clin Invest*. 1994;94:399–404.
34. **Gembal M, Detimary P, Gilon P, Gao ZY, Henquin JC.** Mechanisms by which glucose can control insulin release independently from its action on adenosine triphosphate-sensitive K+ channels in mouse B cells. *J Clin Invest*. 1993;91:871–880.
35. **Rorsman P, Braun M.** Regulation of Insulin Secretion in Human Pancreatic Islets. *Annu Rev Physiol*. 2013;75:155–79.
36. **Buettner R, Scholmerich J, Bollheimer LC.** High-fat diets: modeling the metabolic disorders of human obesity in rodents. *Obesity (Silver Spring)*. 2007;15:798–808.
37. **Braun M, Ramracheya R, Bengtsson M, Zhang Q, Karanauskaite J, Partridge C, Johnson PR, Rorsman P.** Voltage-gated ion channels in human pancreatic beta-cells: electrophysiological characterization and role in insulin secretion. *Diabetes*. 2008;57:1618–1628.
38. **Houamed KM, Sweet IR, Satin LS.** BK channels mediate a novel ionic mechanism that regulates glucose-dependent electrical activity and insulin secretion in mouse pancreatic beta-cells. *J Physiol*. 2010;588:3511–3523.
39. **Jacobson DA, Mendez F, Thompson M, Torres J, Cochet O, Philipson LH.** Calcium-activated and voltage-gated potassium channels of the pancreatic islet impart distinct and complementary roles during secretagogue induced electrical responses. *J Physiol*. 2010;588:3525–3537.
40. **Ammala C, Eliasson L, Bokvist K, Larsson O, Ashcroft FM, Rorsman P.** Exocytosis elicited by action potentials and voltage-clamp calcium currents in individual mouse pancreatic B-cells. *J Physiol*. 1993;472:665–688.
41. **Ivarsson R, Quintens R, Dejonghe S, Tsukamoto K, in 't Veld P, Renstrom E, Schuit FC.** Redox control of exocytosis: regulatory role of NADPH, thioredoxin, and glutaredoxin. *Diabetes*. 2005;54:2132–2142.
42. **MacDonald PE.** Signal integration at the level of ion channel and exocytotic function in pancreatic beta-cells. *Am J Physiol Endocrinol Metab*. 2011;301:E1065–1069.
43. **MacDonald PE, Salapatek AM, Wheeler MB.** Temperature and redox state dependence of native Kv2.1 currents in rat pancreatic beta-cells. *J Physiol*. 2003;546:647–653.
44. **Smith PA, Rorsman P, Ashcroft FM.** Modulation of dihydropyridine-sensitive Ca2+ channels by glucose metabolism in mouse pancreatic beta-cells. *Nature*. 1989;342:550–553.
45. **Maechler P, Wollheim CB.** Mitochondrial glutamate acts as a messenger in glucose-induced insulin exocytosis. *Nature*. 1999;402:685–689.
46. **Laybutt DR, Glandt M, Xu G, Ahn YB, Trivedi N, Bonner-Weir S, Weir GC.** Critical reduction in beta-cell mass results in two distinct outcomes over time. Adaptation with impaired glucose tolerance or decompensated diabetes. *J Biol Chem*. 2003;278:2997–3005.
47. **Jonas JC, Sharma A, Hasenkamp W, Ilkova H, Patane G, Laybutt R, Bonner-Weir S, Weir GC.** Chronic hyperglycemia triggers loss of pancreatic beta cell differentiation in an animal model of diabetes. *J Biol Chem*. 1999;274:14112–14121.
48. **Demidenko ZN, Blagosklonny MV.** Quantifying pharmacologic suppression of cellular senescence: prevention of cellular hypertrophy versus preservation of proliferative potential. *Aging (Albany NY)*. 2009;1:1008–1016.